Process Safety and Environmental Protection, Volume 114, February 2018, pp. 179-191
DOI:10.1016/j.psep.2017.12.018

# Influence of internal fluid velocities and media fill ratio on submerged aerated filter hydrodynamics and process performance for municipal wastewater treatment

Timothy G Holloway[a], Ana Soares[a*]
[a]Cranfield Water Science Institute, Cranfield University, Cranfield, MK43 0AL, UK
Corresponding author: Ana Soares, a.soares@cranfield.ac.uk

## Abstract

Submerged aerated filters (SAFs) treat wastewater to achieve stringent organic carbon and ammonium ($NH_4^+$) effluent consents. Currently SAF design follows a black box approach, where inlet and outlet contaminant concentrations are monitored, with little consideration for internal hydrodynamic conditions. Although tracer tests have been used on bioreactors, integrated monitoring of internal fluid velocities, mixing characteristics and process performance has not been established for SAFs. Tracer tests were performed on a 7.74 $m^3$ SAF, with internal recirculation at 100, 75, 50, 25 and 0% media fill ratios with and without biofilm on the media surface. Results suggested that, SAF internal hydrodynamic conditions directly influenced process performance and media fill ratios could be manipulated to provide optimum conditions for removal of biochemical oxygen demand ($BOD_5$) and $NH_4^+$. A 50% media fill ratio showed optimum hydrodynamic conditions for $BOD_5$ removal, with a removal efficiency of 70% (mass removal of 1.59 $kg.m^{-3}.d^{-1}$). A 100% media fill ratio showed optimum hydrodynamic conditions for $NH_4^+$ removal, with a removal efficiency of 60% (mass removal of 0.14 $kg.m^{-3}.d^{-1}$). Therefore optimisation of internal hydrodynamic conditions is key for selective contaminant removal and achieving high effluent quality.

**Keywords:** Biofilter, Bioreactor, Tracer test, SAF, Wastewater

## 1. Introduction

Submerged aerated filters (SAFs) are well established technologies in treatment of domestic and municipal wastewaters, often used an alternative to conventional biologically aerated filters (BAF) (Moore et al., 2001; Moore et al., 1999). SAF reactors are widely used for secondary and tertiary treatment, with configurations such as upflow, downflow or a combination, when internal recirculation is used (Khoshfetrat et al., 2011; Gálvez et al., 2003). SAF reactors are typically arranged in a series of Cells, with internal dividing baffles to increase treatment efficiency and encourage segregation of heterotrophic and nitrifying processes (Hu et al., 2011). The biofilm grows on a plastic support media, which is submerged in wastewater and can be either, structured or random packed. Media specific surface areas range from 150 to 1200 $m^2.m^{-3}$ with SAFs most commonly using 150 to 600 $m^2.m^{-3}$ (Khoshfetrat et al., 2011; Hu et al., 2011). Aeration of the submerged media is provided by coarse or fine bubble diffusers. Coarse bubble diffusers are often selected over fine, due to the shearing of air bubbles when in contact with the media, which generates a larger mass transfer surface area, similar to that of fine bubbles (Rusten, 1984; Hodkinson et al., 1998). In SAFs with static media contaminant diffusion into the biofilm occurs from a combination of forward fluid velocities ($V_f$) and circulatory mechanisms influenced by aeration.

Internal fluid velocities within SAF reactors have a direct influence over process performance, with high velocities increasing biofilm detachment and washout potential (Burrows et al., 1999). In contrast, low velocities increase solids retention, causing media blinding and reduction in mass transfer efficiency (Priya and Ligy, 2015). Airlift reactors use aeration and a fraction of the flow is constantly recirculated to maintain a stable biofilm thickness. Airlift reactors have two zones, an inner aeration column and an outer draft space. The inner aeration column is raised a nominal distance from the bottom of the reactor. When

aerated, a density difference occurs between inner aeration column and draft space, causing fluid movement through the draft space and into the aeration column (Kilonzo et al., 2006). Therefore changes in draft space baffle position can be used to control recirculation flowrate (Benthum et al., 2000). In fixed film bioreactor engineering, directional fluid movement is typically assumed though strategic aeration described by Rusten et al. (2006).

At high volumetric loadings SAFs suffer from flow shortcutting, therefore it is important to study hydrodynamic properties for optimisation of flow regimes. Biofilm diffusion and dispersion characteristics are influenced by SAF hydrodynamics. This is defined by three parameters; firstly mass transport efficiency (dispersion/advection); secondly mass transfer efficiency (aeration) and thirdly diffusive mass transfer (bulk flow to biofilm). Many studies have been performed using estimations of Peclet number (*Pe*), axial dispersion coefficients (*D*), dispersion number (*d*) and Reynolds number (*Re*) to describe mass transport and transfer dynamics in biofilm reactors (Stevens et al., 1986; Romero et al., 2011; Lamia et al., 2012). Application of these methods would offer insight into how fluid moves and the mass transport dynamics of SAF reactors (Rexwinkel et al., 1997).

In many applications upflow and airlift SAF reactors are preferred due to improved fluid circulation, however the hydrodynamics are not yet fully understood (Pedersen et al., 2015). Most research on SAFs focuses on process efficiency by using variations in the influent wastewater, volumetric and aeration loadings, without considering the internal hydrodynamics conditions (Gálvez et al., 2003; Albuquerque et al., 2012; Bibo et al., 2011). The impact of media fill ratio, internal recirculation, internal baffles, aeration rates and biofilm growth on the media is often excluded from SAF design practices, with commercial design, following a 'black box' approach. The importance of hydrodynamic conditions is investigated in a limited number of studies to date.

Tracer studies are the most established method for analysing reactor hydrodynamic and mixing behaviours. Levenspiel, (1999) completed key research in the application and analysis of tracer studies, establishing many of the parameters used to define hydrodynamic and mixing characteristics in bioreactors. Tracer studies are generally applied to diagnose adverse hydrodynamic conditions in underperforming plant. For example, Christianson et al. (2013) used bromide tracers, in conjunction with dissolved oxygen (DO) and nitrate ($NO_3^-$) analysis to analyse the internal hydraulics of denitrification bioreactors, proving that hydrodynamic performance related to volumetric utilisation within the reactor.

The aim of this research is to investigate the relationship between aeration, media fill ratio and the biofilm to analyse their influence on SAF process performance. Tracer studies were used to investigate internal fluid velocities, mixing and dispersion characteristics. SAF process performance was evaluated by analysing $BOD_5$, $NH_4^+$, total suspended solids (TSS), volatile suspended solids (VSS) and turbidity (NTU) for the duration for the study.

## 2. Materials and methods

### *2.1 Pilot plant*

A SAF pilot plant with a total volume of 7.74 $m^3$ housed two equal Cells: 0.9 m (L) x 1.9 m (W) x 2.1 m (D), with an individual volume of 3.87 $m^3$ (Figure 1). The pilot plant was installed at a municipal wastewater treatment plant for 2840 population equivalent near Bedford, UK. The SAF pilot plant was fed with secondary effluent, processed through secondary trickling filters for $BOD_5$ removal. The wastewater fed to the SAF was delivered by a 0.5 kW, variable speed driven centrifugal pump, calibrated by a fluid velocity probe. Aeration was provided by a 2.6 kW variable speed driven air blower, calibrated by an air velocity probe. With the exception of velocity studies, air was provided at a rate of 21.85

$m^3.h^{-1}.Cell^{-1}$. Coarse bubble air diffusers with 5 mm orifices were pre-installed, having individual velocities of 8.56 $m.s^{-1}$. Three 110 mm pressure distribution holes were provided in each dividing baffle, which allowed flow through the SAF and assisted the inter-baffle down flow of fluid (Figure 1). Random packed polypropylene media was used as a carrier, with a density (ρ) of 1010 $kg.m^{-3}$, specific surface area of 310 $m^2.m^{-3}$, dimensions of 46x36mm and porosity (ε) of 0.9.

The wastewater was fed to the SAF pilot plant at a flow ($Q$) of 2.5±0.07 $m^3.h^{-1}$, giving a hydraulic retention time (HRT) of 184.46 ±1.84 min. The influent characteristics are shown in Table 1. Wastewater samples were taken from the influent, Cell 1, Cell 2 to understand how a series of Cells affects removal efficiency. For this the effluent from each Cell was analysed for $BOD_5$, $NH_4^+$, total phosphorus, alkalinity ($CaCO_3$) TSS and VSS, according to standard methods (American Water Works Association, 1998). Turbidity (NTU) was measured to evaluate, the impact of air scouring on biofilm detachment and retention in Cells. Temperature and dissolved oxygen (DO) measurements were made with Palintest Micro 600, hand held DO and temperature probe, calibrated for each test. Turbidity (NTU) was measured at real time using the fluorometer turbidity channel, calibrated to a standard solution of Rhodamine WT at 5 $mg.l^{-1}$.

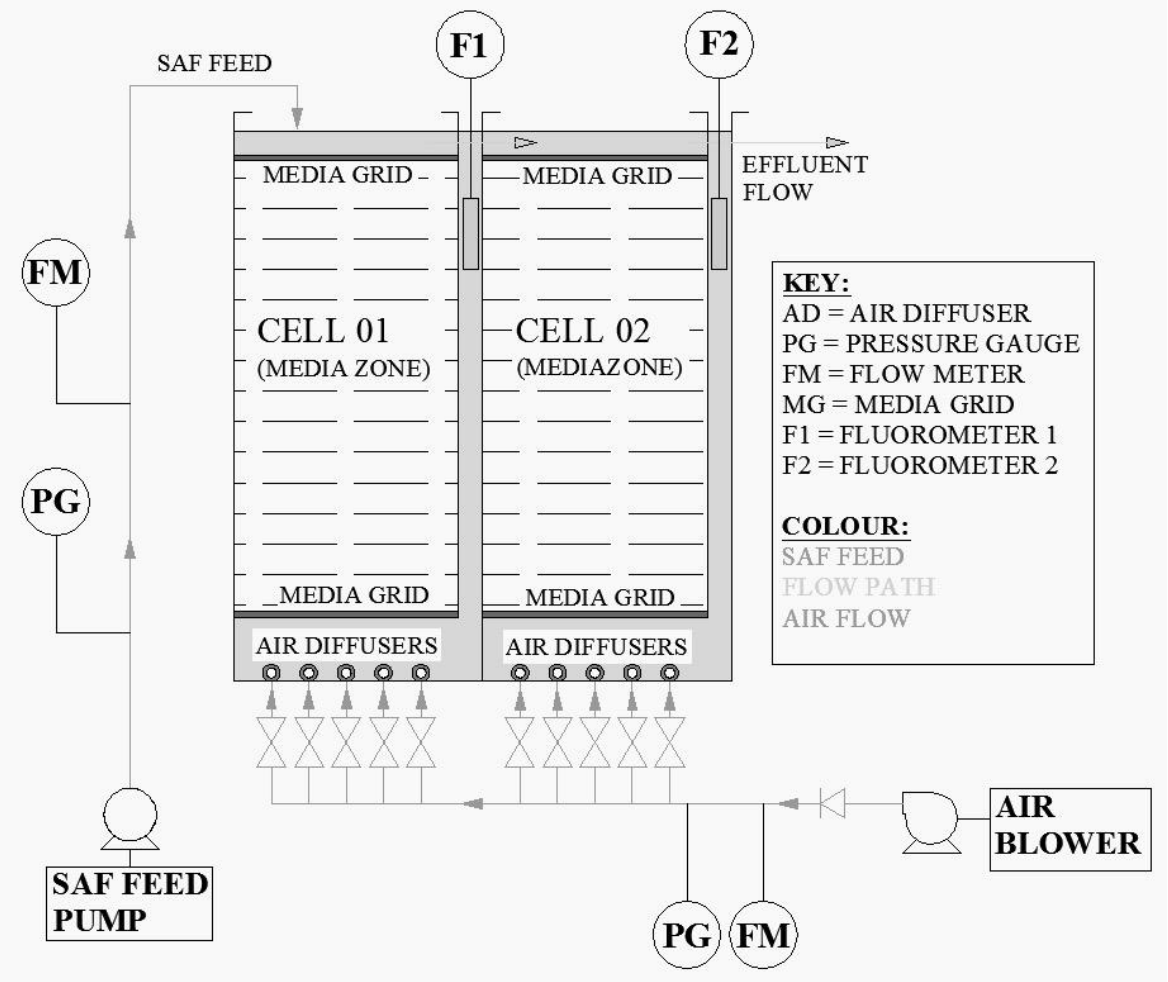


**Figure 1**. Schematic representation of the SAF used to investigate the influence of aeration, media fill ratios, and biofilms on process performance.

5 **Table 1.** Characterisation of the SAF influent wastewater.

| **Parameter** | **Average concentration ($mg.l^{-1}$)*** |
|---|---|
| Ammonium ($NH_4^+$) | 21.0±11.0 |
| $BOD_5$ | 73.0 ±43.0 |
| COD | 152 ± 56.5 |
| $CaCO_3$ | 210.0 ± 91.0 |
| Phosphorus | 6.6 ±1.7 |
| TSS | 101.0 ±31.0 |
| VSS | 56.0 ±1.4 |

*Average of 26 samples. The COD to BOD ratio is 2.1 indicating a biodegradable influent.

### *2.2 Tracer studies*

Rhodamine WT ($C_{29}H_{29}N_2O_5ClNa_2$), 2.5%wt tracer was selected to avoid adsorption issues typically found with Rhodamine B, Lithium chloride and sodium chloride (Teefy, 1996). The tracer was injected into the inlet pipework, using 20 ml syringe with 18 gauge hypodermic needle. Tracer tests on the SAF with, and without biofilm growth, used a full dose of 15.68 ml, whereas velocity studies used a half dose to avoid fluorescence saturation in hourly tracer tests. Fluorometers, with turbidity (NTU) channel and internal data logging were used in the experiments (Turner designs, self contained underwater fluorescence apparatus (SCUFA), California, USA), with a 10s sample interval, and temperature compensation of 0.026/℃. Fluorescence and turbidity channel calibration was performed using a 5 $mg.l^{-1}$ solution of Rhodamine WT, prior to each test.

Tracer studies without biofilm growth were performed with fluorometers positioned within the draft space of both Cells, as detailed in Figure 1. This was done to ensure that the combined flow, including recirculation, was accounted for in the experiments. Each test started with background fluorescence measurement for 1 hr, after which the tracer was injected directly into the inlet pipework, as a pulse, over five seconds, which (Teefy, 1996), describes as instantaneous. Four tracer studies were performed, without biofilm growth on the media, representing increasing hydrodynamic resistance, labelled as 1c to 4c dependent on the level of resistance applied. For the first test the SAF operated on wastewater only to investigate permanent geometries such as baffling (Tracer study 1c); the second test wastewater was aerated at 21.85 $m^3.h^{-1}.Cell^{-1}$ (Tracer study 2c); the third test the SAF was aerated at 21.85 $m^3.h^{-1}.Cell^{-1}$ with internal grids (Tracer study 3c), and in the last test the wastewater was lastly aerated at 21.85 $m^3.h^{-1}.Cell^{-1}$ with, internal grids and 100% media fill ratio (Tracer study 4c). Duplicates were performed for each test for replication of residence

time distribution (RTD) curves. During tracer studies 1c to 4c biofilm was not formed in the media.

Tracer tests were also completed with biofilm growth on the media, during stable operation, when the SAF reached 50 to 100% removal efficiency for $NH_4^+$ and 60 to 100% for $BOD_5$, in accordance with studies by (Peladan et al., 1997) and (Water Environment Federation, 2010). Two replicate tracer tests were performed at 100, 75, 50, and 25% media fill ratios. Injection methods, background fluorescence methods and calculation of ($V_f$) remained the same as SAF without biofilm growth tracer described above. The only difference was extension of the testing period to 13 h to fully account for any tracer retention in stagnant areas of the biofilm on RTD curves as described by Zeng et al., (2013).

Measurement of recirculation flowrate (*Qr*) in the draft space was achieved by mounting two fluorometers in the same Cell on a vertical axis, 1.5 m apart. Recirculation flowrate $Q_r$ ($m^3.s^{-1}$) was calculated from the time taken for the tracer peak to travel the distance between the fluorometers. These tests were performed at aeration rates of 21.85, 32.78 and 43.71 $m^3.h^{-1}.Cell^{-1}$, and for each media fill ratio. Forward tracer velocity ($V_f$) was calculated from the velocity of tracer travelling from Cell 1 to Cell 2 (fluorometer 1 to 2). Media velocities, from 75 to 25% media fill ratio on the fluidised bed were calculated from the time taken for a media element to travel 0.5 m within the Cells.

Residence time distributions (RTDs) are the most common representation of pulse or slug dose tracer tests, with established methods for analysing reactor mixing behaviour. The following parameters were calculated for interpretation of mixing behaviour, resistive and dispersion dynamics (Levenspiel, 1999). Equation 1 and 2 relate directly to RTD curves, with Equation 1 describing the tracer retention in the vessel, independent of the hydraulic retention time (HRT), and Equation 2 the spread of the curve, giving indication of mixing efficiency. The $n\text{-}_{CSTR}$ equation is used for defining the extent that bioreactors operate in either CSTR or

PFR as shown in Equation 3, which is also reflected in Equation 4, but based on probabilistic tracer elution. Volumetric efficiency (*Ve*), shown in Equation 5 estimates the volumetric utilisation of a reactor. Dispersion and advection are most commonly predicted, using *Pe* shown in Equation 8, with axial dispersion predicted by D in Equation 7, taking units of $m^2.s^{-1}$. Reynolds number is used to describe the flow regime and its variation from laminar or turbulent conditions shown in Equation 10.

$$\bar{t} = \frac{\int_0^\infty t\, C(t)\, dt}{\int_0^\infty C(t)\, dt} \qquad \text{(Equation 1)}$$

Where t is time, *C(t)* is tracer concentration with respect to *t*, and $\bar{t}$ is the mean residence time, based on the tracer response (Levenspiel, 1999) (Equation 1).

$$\sigma^2 = \frac{\int_0^\infty t^2\, C(t)\, dt}{\int_0^\infty C(t)\, dt} - \bar{t}^2 \qquad \text{(Equation 2)}$$

Where $\sigma^2$ ($min^{-1}$) is the spread of the RTD, based on the tracer response within the reactor and defining the back-mixing efficiency. Therefore large values (>4000) show elongated tracer curve, with an even distribution over the RTD curve. Low (<1500) values indicate a large peak on the RTD and thus slewing the variance (Teefy, 1996) (Equation 2).

$$n_{-CSTR} = \frac{\bar{t}^2}{\sigma^2} \qquad \text{(Equation 3)}$$

Where $n\text{-}_{CSTR}$, is the number of continuously stirred tank reactors (CSTR) in series. When $n\text{-}_{CSTR} = 1$, the bioreactor is considered an efficient CSTR, a $n\text{-}_{CSTR} > 1$ indicates hybrid behaviour between a CSTR and plug flow reactor (PFR), and $n\text{-}_{CSTR} = 30$, indicates an ideal PFR (Burrows et al., 1999) (Equation 3).

$$MDI = \frac{P_{90}}{P_{10}} \qquad \text{(Equation 4)}$$

Morril dispersion index (*MDI*) is based on the probabilistic tracer elution from a reactor, with 90% ($P_{90}$) and 10% ($P_{10}$). A value of 2 or less is considered an efficient PFR, and 22 a CSTR (Tchobanoglous et al., 2003) (Equation 4).

$$V_e = \frac{1}{MDI} \times 100 \qquad \text{(Equation 5)}$$

Where $V_e$ the volumetric efficiency of the reactor that provides estimation of the actively mixed zone within a reactor (Tchobanoglous et al., 2003) (Equation 5).

$$\sigma_\theta^2 = \frac{\sigma^2}{\bar{t}^2} \qquad \text{(Equation 6)}$$

Where $\sigma_\theta^2$ is the normalised variance for a closed vessel, based on fluid entering and exiting the SAF under laminar flow conditions. It is the inverse of $n_{\text{-}CSTR}$ and typically used in conjunction with Equation 7 (Levenspiel, 1999) (Equation 6).

$$\sigma_\theta^2 = 2\left(\frac{D}{uL}\right) - 2\left(\frac{D}{uL}\right)^2\left[1 - e^{-uL/D}\right] \qquad \text{(Equation 7)}$$

Where $D$ is the axial dispersion coefficient, $L$ is the characteristic length over which dispersion occurs and $u$ the velocity. As in Equation 6 $\sigma_\theta^2$ is used as the basis for iterative calculations for estimation of the axial dispersion coefficient $D$ (Levenspiel, 1999) (Equation 7).

$$P_e = \frac{uL}{D} \qquad \text{(Equation 8)}$$

Where $P_e$ is the Peclet number that defines the mass transport mechanism, either dispersion or advection (Molecular diffusion or flow transportation). Values greater than 1 indicate advection, and less than 1 dispersion (Doran, 2013) (Equation 8).

$$d = \frac{D}{uL} \quad \text{(Equation 9)}$$

Where $d$ is the inverse of $Pe$ representing the extent of dispersion in the bioreactor (Tchobanoglous et al., 2003) (Equation 9).

$$Re = \left(\frac{Sh}{0.026\ Sc^{0.3}}\right)^{\left(\frac{1}{0.8}\right)} \quad \text{(Equation 10)}$$

Where *Re* is the Reynolds number, *Sh* is the Sherwood number and *Sc* is the Schmidt number, used to characterise flow dynamics in the horizontal plane (Zhu and Chen, 2001) (Equation 10).

## 3. Results and discussion

### *3.1 Tracer tests on SAF without biofilm growth*

Tracer tests were completed without biofilm growth to investigate the influence of internal SAF components on hydrodynamic conditions, demonstrated in the RTD curves (Figure 2a and b). Fluorescence measurements were collected from Cell 1 and 2, with Figure 2a showing RTD curves for the SAF fed continuously with wastewater (Table 2, 1c), and Figure 2b the SAF operated with aeration, internal grids and 100% media fill ratio (Table 2, 4c). Tracer peaks in Cell 1 occurred shortly after entry (6.16 min), with sharp tracer peaks lasting one sample period (10s). The RTDs differ from that observed in other studies (Zeng et al., 2013; Seifert and Engesgaard, 2007; Ahnert et al., 2010), where RTDs approached Gaussian

symmetry. The sharp tracer peaks observed in the SAF indicated flow shortcutting through the 110mm holes in the dividing baffles, indicated by $\bar{t}$ remaining lower than τ in all tracer studies (Table 2).

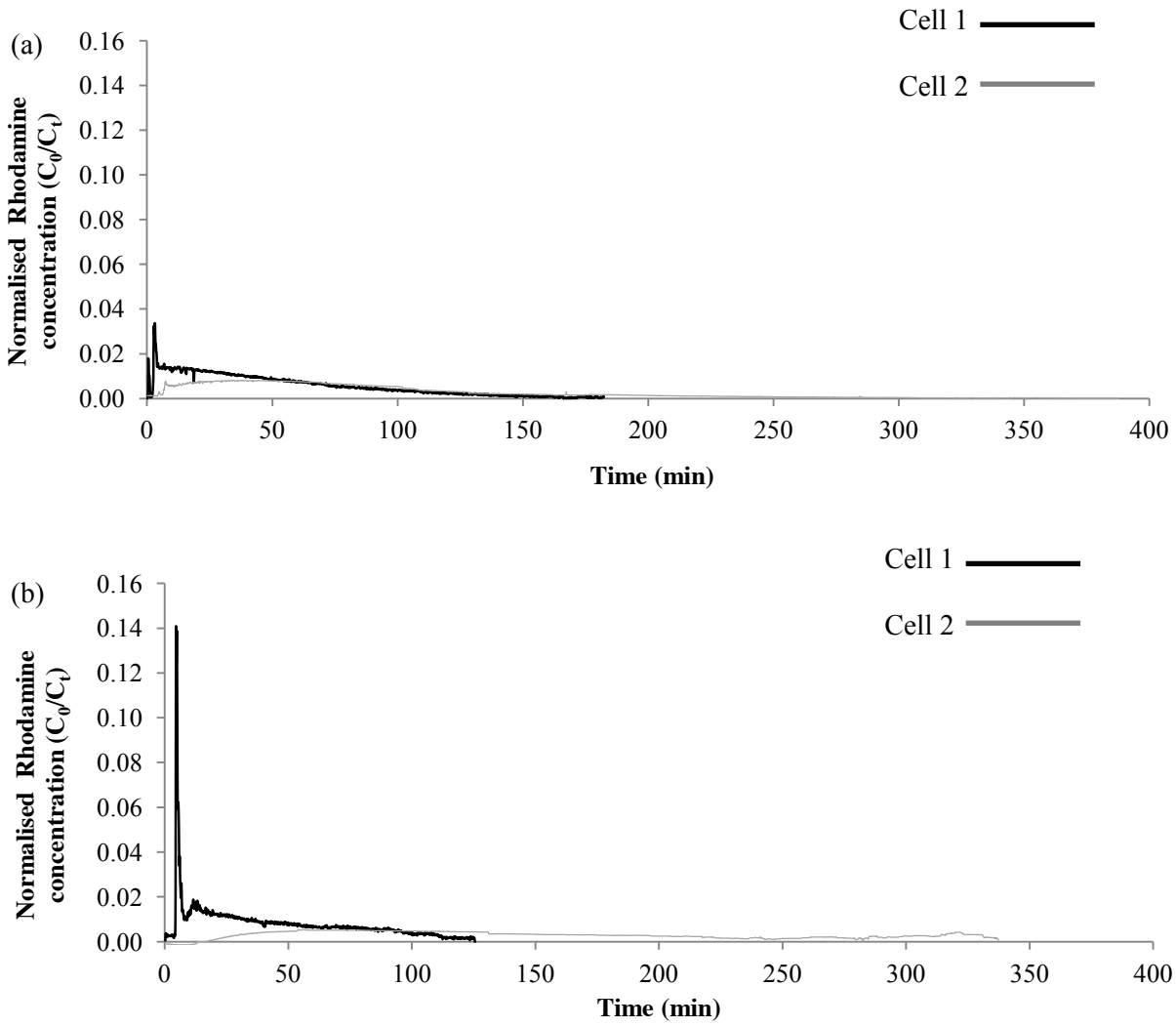


**Figure 2.** Example RTD when the SAF was fed continuously at 2.5±0.07 $m^3.h^{-1}$, without aeration, internal grids or media *(a)* and with 100% media fill ratio, internal grids and aeration at a rate of 21.85 $m^3.h^{-1}.Cell^{-1}$ *(b)*.

In tracer study 2c (Table 2), the SAF operated with aeration, but without internal grids and media. The value for $\bar{t}$ was 35.97 min in Cell 1 and 93.61 min for Cell 2, demonstrating a loss of 55 and 89 min from $\tau$ in Cell 1 and 2 respectively. Therefore aeration increased flow

shortcutting, reducing tracer retention within the *SAF* Cells. This also agrees with the tracer travel time ($T_t$), which was lowest of all tracer studies at 27 min and $V_f$ at 2.3 m.h$^{-1}$ (Table 2). *MDI* showed a further shift toward an ideal *PFR* (*MDI* = 1) conditions at 1.74 and 1.72 for Cell 1 and 2 respectively (Tchobanoglous et al., 2003). This indicates increased fluid velocities in the upper zone of the SAF, transporting tracer within the flow. *Pe* values doubled, shifting mass transport toward advection and was also evident in *D* and *d*, which halved, correlating with the *MDI*.

In tracer study 3c, the SAF was operated with aeration, internal grids, but without media. Values for $\bar{t}$ were still below $\tau$ by 16 min and 57.5 min for Cell 1 and 2 respectively, meaning internal grids improved tracer retention from tracer study 2c (Table 2). The $\sigma^2$ increased from 3085 and 6929 min$^{-1}$ passing from Cell 1 to 2 and *Ve* from 49 to 63% respectively, indicating a distinct increase in tracer distribution over the RTD and hence mixing efficiency. Both Cells operated as an efficient PFR (*MDI* $\leq$ 2), demonstrating improvement in PFR characteristics over the successive SAF Cells. Pe, aligned with $\sigma^2$ and $V_e$, indicates a shift toward dispersion with a reduction from 2c (Table 2) to 0.0401 and 0.0554 in Cell 1 and 2, respectively.

For tracer study 4c the SAF operated with aeration, internal grids and 100% media fill ratio. Values of $\bar{t}$ was 51 min below $\tau$ in Cell 1 and 32 min in Cell 2, therefore flow shortcutting did occur in Cell 1. However $\bar{t}$ increased to the longest tracer retention for Cell 2 at 153 min. The square of the variance corresponded with the reduction in $\bar{t}$ from tracer study 3c (Table 2), falling to 1054 min$^{-1}$ in Cell 1, indicating inefficient back-mixing. However, Cell 2 displayed the largest value of all tests completed without biofilm growth at 8059 min$^{-1}$. Therefore, although mixing in Cell 1 appeared inefficient ~~it improved~~ as it passed to Cell 2, which was also evident in the increased tracer travel to 50 min and reduction in $V_f$ to 1.24

m.h$^{-1}$. In-line with $\sigma^2$ Cell 1 showed CSTR characteristics (*MDI* >2), with an *MDI* of 2.75, but Cell 2 at 1.46, demonstrates that a series of cells shift dynamics toward PFR (Levenspiel, 1999). This was also evident in *Pe*, increasing from 0.0308 in Cell 1, to 0.0767 in Cell 2 and hence corresponding with a reduction in *d* from 32.36 to 13.03 in Cell 2. *Re* reduced in both Cells from tracer study 3c to 927 and 963 for Cell 1 and 2, again due to laminar flow in the upper zone of the SAF. Overall aeration, internal grids and media improved tracer dispersion in Cell 1, which agrees with the studies completed by Priya and Ligy, (2015) and Hodkinson et al. (1998).

**Table 2:** Hydrodynamic parameters calculated from the tracer tests in the SAF pilot plant without biofilm growth on the media surface, where $\tau$ is theoretical detention time, $\bar{t}$ is the mean residence time, $\sigma^2$ is the square of the variance, *Ve* is the volumetric efficiency, $T_t$ is the tracer travel time from Cell 1 to 2, $V_f$ is the forward velocity of tracer passing from Cell 1 to 2, *MDI* is the Morril dispersion index, *n-CSTR* is the number of continuously stirred tank reactors, *D* is the axial dispersion coefficient, *d* is the dispersion number, *Pe* is the Peclet number, *Re* is the Reynolds number based on forward velocity.

| Tracer study | Parameter | $\tau$ (min) | $\bar{t}$ (min) | $\sigma^2$ (min$^{-1}$) | *Ve* (%) | Peak $C_i/C_t$ | $T_t$ (min) | $V_f$ (m.h$^{-1}$) | *MDI* | *n-CSTR* | *Pe* | *D* (m$^2$.s$^{-1}$) | *d* | *Re* |
|---|---|---|---|---|---|---|---|---|---|---|---|---|---|---|
| **1c** | SAF, wastewater only, Cell 01 | 92.24 | 54.03 | 1533.20 | 51.22 | 0.032 | - | - | 1.96 | 1.91 | 0.0388 | 0.0170 | 25.82 | 1187.81 |
| | SAF, wastewater only, Cell 02 | 184.48 | 94.29 | 5471.44 | 57.61 | 0.008 | 41.50 | 2.33 | 1.74 | 1.63 | 0.0277 | 0.0240 | 35.98 | 1171.46 |
| **2c** | SAF, wastewater, aeration, Cell 01 | 91.35 | 35.97 | 459.44 | 57.54 | 0.025 | - | - | 1.74 | 2.82 | 0.0723 | 0.0090 | 13.85 | 1213.27 |
| | SAF, wastewater, aeration, Cell 02 | 182.70 | 93.61 | 2890.41 | 58.43 | 0.001 | 26.60 | 2.30 | 1.72 | 3.04 | 0.0813 | 0.0080 | 12.31 | 1219.24 |
| **3c** | SAF, wastewater, aeration, grids, Cell 01 | 92.34 | 77.15 | 3085.01 | 49.44 | 0.021 | - | - | 2.03 | 1.93 | 0.0401 | 0.0145 | 24.95 | 1135.11 |
| | SAF, wastewater, aeration, grid, Cell 02 | 184.68 | 127.18 | 6929.87 | 63.81 | 0.006 | 29.83 | 2.06 | 1.57 | 2.34 | 0.0554 | 0.0105 | 18.07 | 1150.48 |
| **4c** | SAF, wastewater, grid, 100% media fill ratio, Cell 01 | 93.21 | 42.30 | 1054.97 | 36.36 | 0.141 | - | - | 2.75 | 1.69 | 0.0308 | 0.0113 | 32.36 | 927.45 |
| | SAF, wastewater, grid, 100% media fill ratio, Cell 02 | 186.42 | 153.79 | 8059.72 | 68.27 | 0.005 | 49.67 | 1.24 | 1.46 | 2.94 | 0.0767 | 0.0045 | 13.03 | 963.28 |

### *3.2 Tracer tests on SAF with biofilm growth*

Tracer tests were also completed when the media was fully colonised with biofilm, to investigate influence of biofilm on SAF hydrodynamics and demonstrated in RTDs (Figure 3a and b). Fluorescence measurements were collected from exit of Cell 1 and 2 (Figure 1), with Figure 3a showing RTDs curves for the SAF was fed continuously, with aeration, internal grids and 100% media fill ratio and Figure 3b the SAF operated with aeration, internal grids and 25% media fill ratio. The tracer peak in Cell 1 ~~in (~~Figure 3a) occured shortly after tracer entry (2.66 min) lasting one sample period, whereas Figure 3b shows elimination of the sharp tracer peak, occurring at (12.66 min) and a more balanced distribution over the RTD. This is similar to observed by Davidson et al., (2008) and Stevens et al. (1986) in tracer studies of fluidised bed sand filters. As media was removed from 75 to 25% the media progressively fluidised with complete fluidisation occurring at 25% media fill ratio.

From the RTDs produced, hydrodynamic and dispersion parameters were calculated (Table 3). In tracer study 1b (Table 3) the SAF was operated with aeration, internal grids, 100% media fill ratio and biofilm on the media surface. Values for $\bar{t}$ remained below $\tau$ by 25.89 min in Cell 1, and 44 min in Cell 2, again indicating flow shortcutting. $\sigma^2$ increased from 3062 in Cell 1 to 6311 in Cell 2, indicating a balanced increase in back-mixing mixing efficiency. The *MDI* showed an increase in CSTR characteristics from tracer study 4c, with a value of 3.94 in Cell 1. However, Cell 2 with a value of 1.46, displayed similar PFR characteristics to tracer study 4c. *Pe* increased in a similar way to tracer study 4c, from 0.019 to 0.084 from Cell 1 to 2, corresponding with the reductions in D and d. It is clear from the results that mass transport varies between Cell 1 and 2 and confirms observations made by Levenspiel, (1999) where a series of cells simulates PFR conditions.

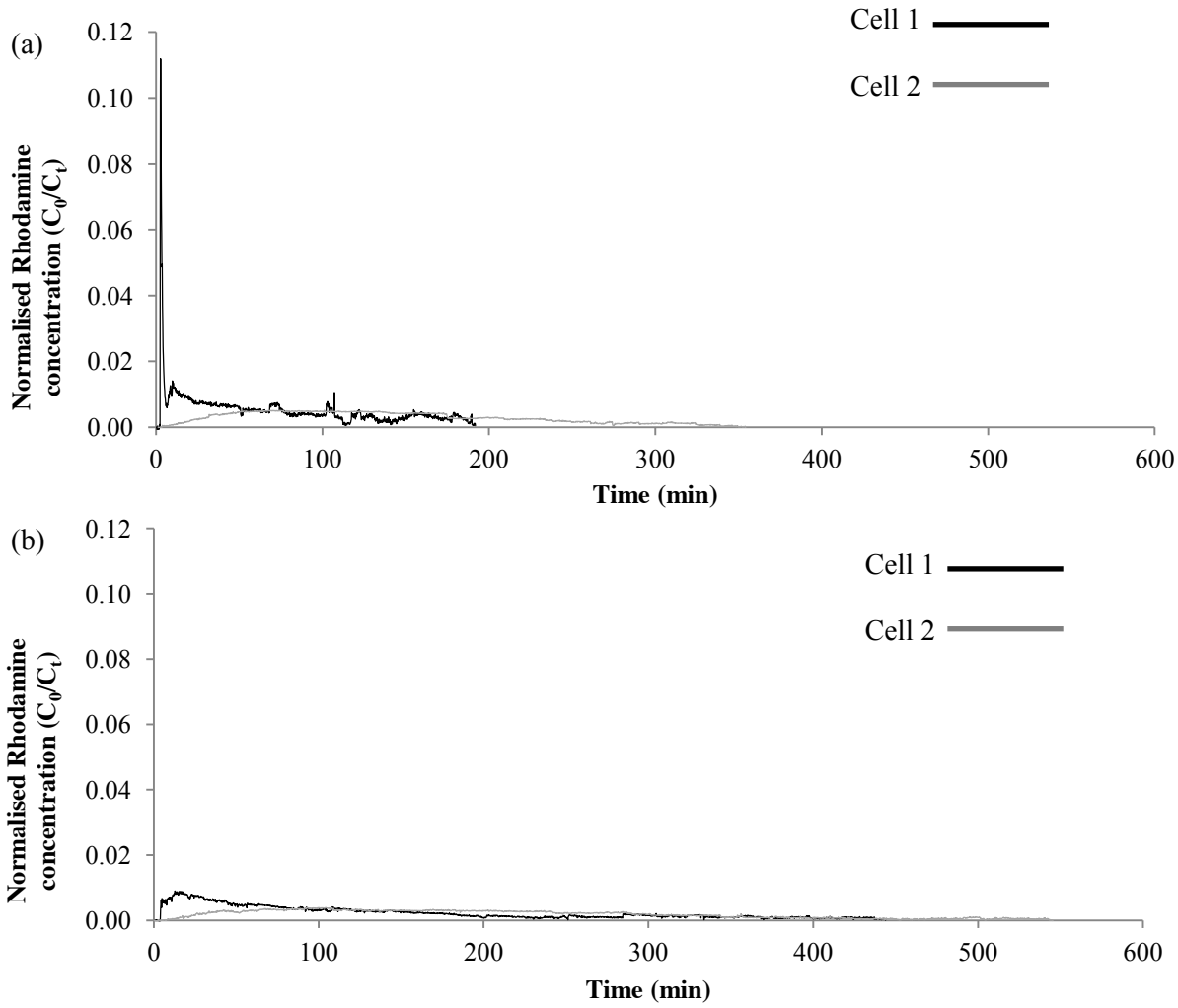


**Figure 3.** Example RTD curves when the SAF was fed continuously at was 2.5 ±0.07 $m^3.h^{-1}$, with100% media fill ratio, internal grids and aeration rate of 21.85 $m^3.h^{-1}.Cell^{-1}$, *(a)* and with 25% media fill ratio, internal grids and aeration at 21.85 $m^3.h^{-1}.Cell^{-1}$.

In tracer study 2b the SAF was operated with aeration, internal grids, 75% media fill ratio and biofilm on the media surface. Values for $\bar{t}$ was below τ by 29 min in Cell 1 and 19 min in Cell 2. Therefore, although flow shortcutting occurred in Cell 1, the media circulation at 75% media fill ratio reduced the differential between $\bar{t}$ and τ in Cell 2. This is also reflected in $\sigma^2$, which increased from 2204 to 9113 $min^{-1}$ as tracer moved from Cell 1 to 2. $V_f$ showed lowest value of all studies at 0.42 $m.h^{-1}$ as it passed from Cell 1 to 2, indicating that tracer was retained within the Cells, becoming entrained in the circulating media. *Pe* increased from 0.035 in Cell 1 to 0.080 in Cell 2, similar to tracer study 1b. The most notable change occurred with *D* in Cell 2 to with the lowest value of all studies at 0.0015,

demonstrating lowest axial tracer movement. Re showed the lowest values of all studies at 620 and 642 for Cell 1 and 2 respectively, meaning it is seemingly laminar due to the reduction in $V_f$ and media entrainment.

In tracer study 3b the SAF was operated with aeration, internal grids, 50% media fill ratio and biofilm on the media surface. The value of $\bar{t}$ exceeded $\tau$ by 68 min in Cell 1 and 69 min in Cell 2 (Table 3). Therefore, tracer retention increased and was consistent across both Cells, indicating prolonged biofilm contact. This was also evident in $\sigma^2$, which increased significantly from 11103 to 29917 $min^{-1}$ from Cells 1 to 2. *MDI* displayed similar values, close to ideal PFR characteristics, in both SAF Cells, indicating balanced hydrodynamic conditions (Tchobanoglous et al., 2003). The $V_e$ showed the largest value of all studies in Cell 1 and 2 at 60% and 67% respectively, demonstrating improved volumetric utilisation within the SAF, with balanced hydrodynamic conditions in both cells. $T_t$ increased to 90 min, which was the highest of all studies, demonstrating an increased retention of tracer. *Pe* values showed similar conditions between Cell 1 and 2 at 0.054 and 0.049 respectively, corresponding to balanced *D* and *d*, indicating similar hydrodynamic conditions in both Cells. *Re* increased slightly from tracer study 2b to 754 and 751 for Cell 1 and 2 respectively, demonstrating similar internal resistance.

**Table 3:** Hydrodynamic parameters calculated from the tracer tests in the SAF pilot plant with biofilm growth on the media surface, where $\tau$ is theoretical detention time, $\bar{t}$ is mean residence time, $\sigma^2$ is the square of the variance, *Ve* is the volumetric efficiency, $T_t$ is the tracer travel time from Cell 1 to 2, $V_f$ is the forward velocity of tracer passing from Cell 1 to 2, *MDI* is the Morril dispersion index, *n-CSTR* is the number of continuously stirred tank reactors, *D* is the axial dispersion coefficient, *d* is the dispersion number, *Pe* is the Peclet number, *Re* is the Reynolds number based on forward velocity.

| **Tracer study** | **Parameter** | $\tau$ **(min)** | $\bar{t}$ **(min)** | $\sigma^2$ **(min$^{-1}$)** | $V_e$ **(%)** | **Peak, ($Ci/C_t$)** | $T_t$ **(min)** | $V_f$ **(m.h$^{-1}$)** | ***MDI*** | ***n-CSTR*** | ***Pe*** | ***D*** **(m$^2$.s$^{-1}$)** | ***d*** | ***Re*** |
|---|---|---|---|---|---|---|---|---|---|---|---|---|---|---|
| **1b** | SAF, 100% media fill ratio, Cell 01 | 92.05 | 66.16 | 3062.02 | 25.34 | 0.111 | - | - | 3.94 | 1.42 | 0.019 | 0.0089 | 50.84 | 704.05 |
| | SAF, 100% media fill ratio, Cell 02 | 184.10 | 140.60 | 6311.10 | 68.75 | 0.005 | 67.83 | 0.63 | 1.46 | 3.14 | 0.084 | 0.0021 | 11.93 | 747.9 |
| **2b** | SAF, 75% media fill ratio Cell 01 | 92.65 | 63.20 | 2204.30 | 43.53 | 0.020 | - | - | 2.30 | 1.82 | 0.035 | 0.0034 | 28.25 | 620.13 |
| | SAF, 75% media fill ratio Cell 02 | 185.30 | 166.30 | 9113.43 | 66.67 | 0.004 | 71.99 | 0.42 | 1.50 | 3.04 | 0.080 | 0.0015 | 12.47 | 641.63 |
| **3b** | SAF, 50% media fill ratio Cell 01 | 92.07 | 159.80 | 11103.24 | 60.25 | 0.006 | - | - | 1.66 | 2.30 | 0.054 | 0.0036 | 18.58 | 754.81 |
| | SAF 50% media fill ratio Cell 02 | 184.10 | 253.60 | 29917.39 | 66.73 | 0.004 | 89.83 | 0.74 | 1.50 | 2.15 | 0.049 | 0.0040 | 20.69 | 751.43 |
| **4b** | SAF, 25% media fill ratio Cell 01 | 92.1 | 134.61 | 13509.40 | 50.21 | 0.009 | - | - | 2.00 | 1.35 | 0.017 | 0.0121 | 60.6 | 732.77 |
| | 25% media fill ratio Cell 02 | 184.20 | 201.42 | 15037.82 | 66.73 | 0.004 | 86.84 | 0.71 | 1.50 | 2.70 | 0.073 | 0.0028 | 13.88 | 779.2 |

In tracer study 4b, the SAF was operated with aeration, internal grids, 25% media fill ratio and biofilm on the media surface. Values of $\bar{t}$ exceeded $\tau$ by 43 min in Cell 1 and 17 min in Cell 2, which is a significant reduction from tracer study 3b (50% media fill ratio). The square of the variance increased in Cell 1 from tracer study 3b to 13509 $min^{-1}$ and reduced in Cell 2 to 15037 $min^{-1}$, demonstrating little improvement in mixing between Cell 1 and 2. The *MDI* indicated *PFR* conditions in both Cells at 2 and 1.5 respectively, but *Ve* reduced to 50% from tracer study 3b, indicating an imbalance in hydrodynamic conditions between cells. *Pe* showed the lowest value of all studies in Cell 1 at 0.017, corresponding with *D* and d at 0.0121 $m^2.s^{-1}$ and 60.6 respectively. Conversely, *Pe* increased in Cell 2 to 0.073, in line with six fold reductions for D and d. Therefore dispersion was dominant in Cell 1 and Cell 2 moved towards advection. Therefore variations in mass transport mechanisms between Cell 1 and 2, related to changes in mixing and dispersion, thus affecting process dynamics.

### *3.3 Internal recirculation tracer tests*

When the SAF was operated with 100% media fill ratio it showed lowest volumetric internal recirculation rate ($Q_r$) at 4.37, 7.94 and 16.55 $m^3.h^{-1}$ for aeration rates of 22.16, 33.05 and 43.92 $m^3.h^{-1}.Cell^{-1}$. Therefore corresponding with high dispersion seen in tracer study 1b where *d* was 50.84 and *MDI* was 3.94 (CSTR) for Cell 1 (Table 3). Therefore aeration and dispersed tracer throughout the fixed 100% filled media bed, caused recirculation resistance in the Cells (Hodkinson et al., 1998). Media elements started to fluidise at 75% media fill ratio, with a reordering velocity of 0.0058 $m.s^{-1}$ (Table 3). A linear increase in *Qr* occurred at 75% media fill ratio with an aeration rate of 22.08 $m^3.h^{-1}.Cell^{-1}$ similar to 100% media fill ratio at 4.23 $m^3.h^{-1}$. As the aeration rate was increased to 32.85 and 43.74 $m^3.h^{-1}.Cell^{-1}$ recirculation rate increased to 13.38 and 21.47 $m^3.h^{-1}$. This corresponds with the lowest $V_f$

value of all studies at 0.42 $m.h^{-1}$, a reduction of Re to 620 and 641 for Cell 1 and 2 respectively (Table 3). Moreover $\sigma^2$ increased to 9113 in Cell 2, demonstrating that media re-ordering reduced recirculation resistance within the SAF and *Qr* increased, along with tracer retention.

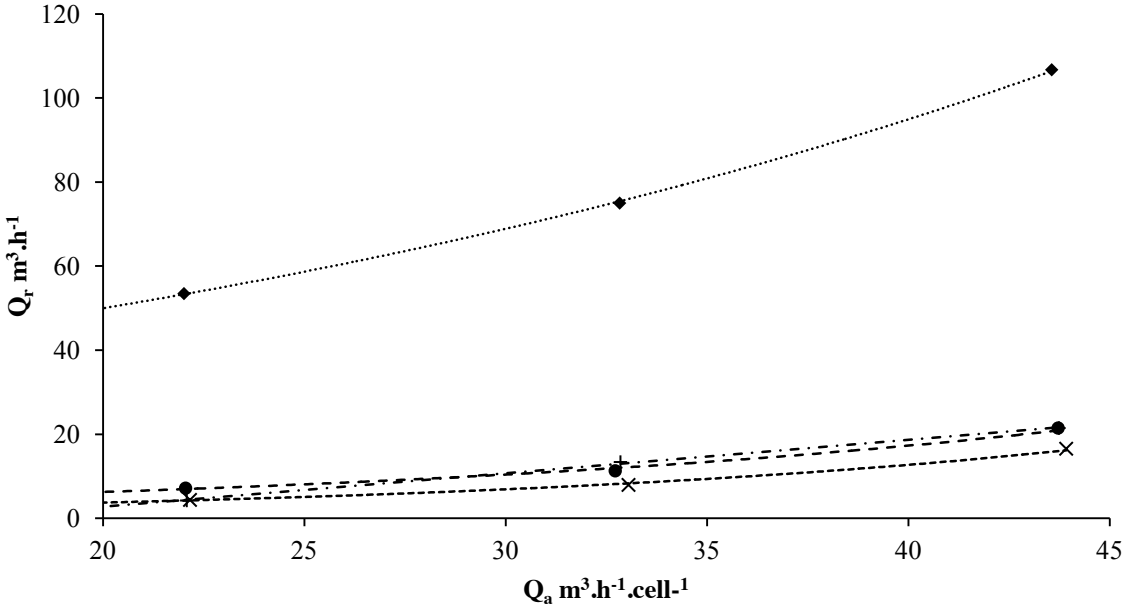


**Figure 4.** Influence of aeration rate ($Q_a$) on the SAF internal recirculation (Qr - volumetric recycle flowrate) on the SAF with 100% media fill ratio (×), 75% media fill ratio (+), 50% media fill ratio (•) and 25% media fill ratio (♦). The SAF was fed at 2.5 ±0.07 $m^3.h^{-1}$, and aerated at between 21.85 and 43.7 $m^3.h^{-1}.Cell^{-1}$. Fluorometers were mounted vertically within the draft space for Cell 1, 1.5m apart.

Moderate media fluidisation occurred at 50% media fill ratio, with increased media element collisions and velocities of 0.301 $m.s^{-1}$ (Table 4). The *Qr* increased from 75% media fill ratio to 7.16 $m^3.h^{-1}$ from 75% when aerated at 22.05 $m^3.h^{-1}.Cell^{-1}$. Although, when aerated at 32.72 $m3.h^{-1}.Cell^{-1}$ *Qr* reduced to 11.29 $m^3.h^{-1}$ and when aerated at 43.72 $m^3.h^{-1}.Cell^{-1}$ the same *Qr* as 75% media fill ratio was seen at 21.47 $m^3.h^{-1}$. This suggests that, although *Qr* increased from 75% media fill ratio when aerated at 22.05 $m^3.h^{-1}.Cell^{-1}$, *Qr* increased exponentially as displayed in Figure 4. Complete media element fluidisation occurred at 25% media fill ratio, showing a 43.6 $m^3.h^{-1}$ increase in $Q_r$ from 50% media fill ratio. This was demonstrated by the largest dispersion values of all studies, with *d* and *D* at 60.6 and 0.0121

respectively for Cell 1 (Table 3). Therefore media elements provided little resistance to upward aeration velocity and thus the recirculation rate increased. This aligns with the findings of Wang et al., (2005), who investigated aeration requirements for media element fluidisation. With the exception of 75% media fill ratio (Figure 4), which showed a linear relationship, all other media fill ratios displayed exponential curves. Therefore predictions of *Qr* can be made by inputting *Qa* into the equations shown in Table 4.

**Table 4.** Internal media velocities $V_m$, at aeration rates of 21.8, 32.78 and 43.72 $m^3.h^{-1}.Cell^{-1}$ and media movement, with equations for prediction of *Qr*.

| **Study conditions** | **Media movement** | $V_m$ **(m.s$^{-1}$)* Qa =21.86 (m$^3$.h$^{-1}$.Cell$^{-1}$)** | $V_m$ **(m.s$^{-1}$)* Qa =32.78 (m$^3$.h$^{-1}$.Cell$^{-1}$)** | $V_m$ **(m.s$^{-1}$)* Qa =43.72 (m$^3$.h$^{-1}$.Cell$^{-1}$)** | **$Q_r$ (prediction)** |
|---|---|---|---|---|---|
| 100% media fill ratio with biofilm | Fixed | 0 | 0 | 0 | $Q_r = 1.1004e^{0.0612Q_a}$ |
| 75% media fill ratio with biofilm | Re-ordering | 0.006 | 0.008 | 0.017 | $Q_r = 0.7958Qa - 13.148$ |
| 50% media fill ratio with biofilm | Moderate fluidisation | 0.301 | 0.465 | 0.641 | $Q_r = 5.1391e^{0.0318Q_a}$ |
| 25% media fill ratio with biofilm | Complete fluidisation | 0.319 | 0.304 | 0.284 | $Q_r = 26.316e^{0.0321Q_a}$ |

* Average of 12 measurements.

***3.4 Effect of media fill ratio on process performance***

When the SAF reached stable operation the process performance was investigated for each media fill ratio tested (Figure 5). Figure 5a shows the influence of media fill ratio on $BOD_5$ and $NH_4^+$ removal efficiencies and Figure 5b shows the organic loading rate for each media fill ratio. At 100% and 25% media fill ratio removal efficiency for $BOD_5$ was 79 and 78% respectively (Figure 5a). However 50% media fill ratio the SAF encountered the highest organic loading rate at 3.13 $kg.m^2.d^{-1}$, leading to reduced removal efficiency of 70%, but removing a larger mass of $BOD_5$ at 2.2 $kg.m^2.d^{-1}$. Moreover this corresponds with the balanced hydrodynamic conditions, whereby $\bar{t}$ exceeded $\tau$ by approximately 70 min in both

Cells, and *Ve*, *Pe*, *D* and *MDI* displayed similar values in both Cells, hence displaying balanced dispersion characteristics (Table 3). This agrees with Wang et al., (2005), where 50% media fill ratio is defined as optimum and 73% COD removal was observed.

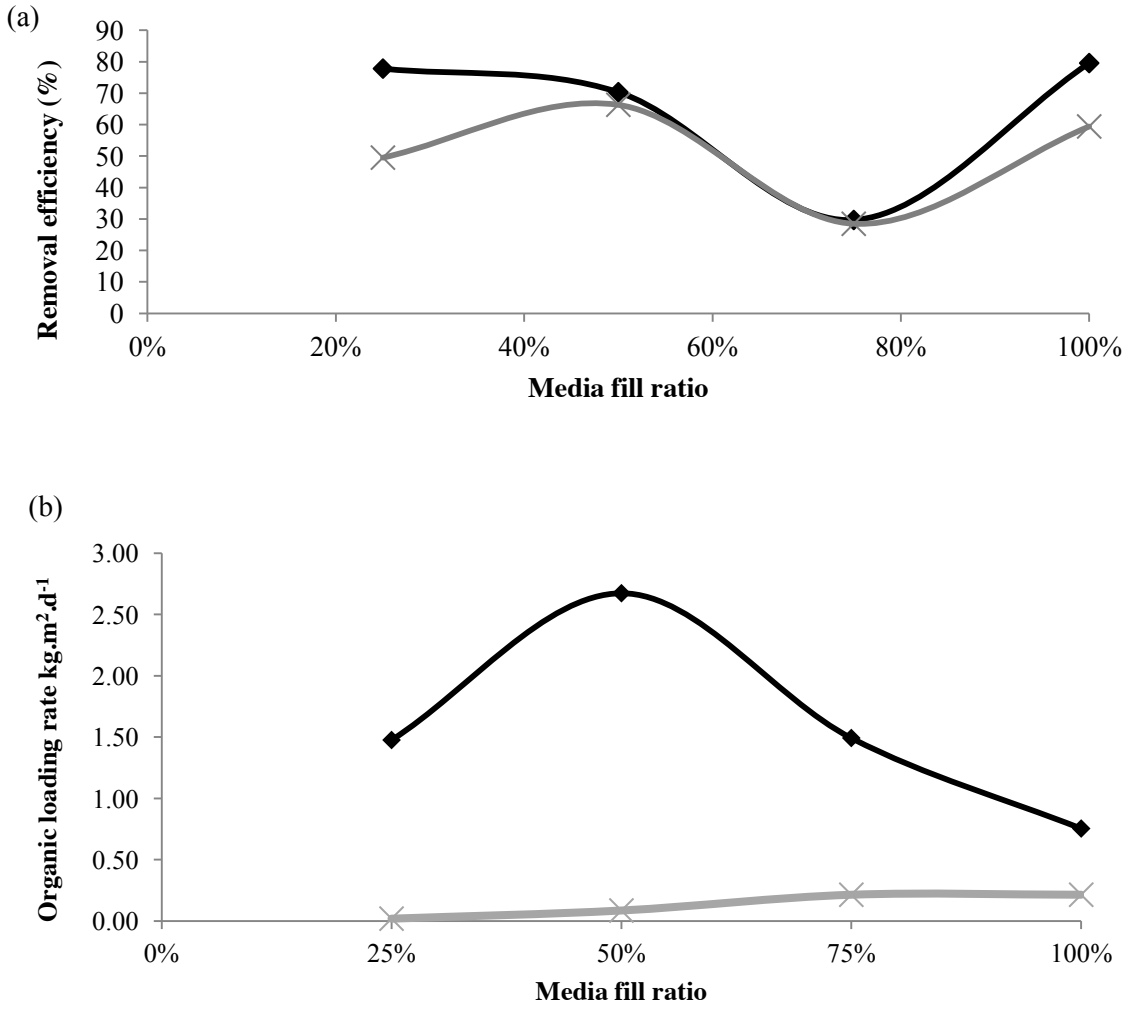


**Figure. 5.** Removal efficiency and organic loading rate to the SAF, tested for 100, 75, 50 and 25% media fill ratio. Where (a) is the average efficiency and (b) organic loading rate, with $BOD_5$ (♦) and $NH_4^+$ (×). The SAF was fed at 2.5 ±0.07 $m^3.h^{-1}$, with an aeration rate of 21.85 $m^3.h^{-1}.Cell^{-1}$.

At 100% and 50% media fill ratio the SAF achieved the highest $NH_4^+$ removal efficiencies of 60 and 66% respectively (Figure 5a). On the other side, the removal efficiency was reduced to 60% at 100% media fill ratio, the elevated organic loading rate of 0.42 $kg.m^2.d^{-1}$ resulted in a higher mass removal of $NH_4^+$ at 0.252 $kg.m^2.d^{-1}$. The low removals at

75% media filling ratio can be explained through the data obtained in the hydraulic study. Although 75% media fill ratio had the lowest $V_f$, ($V_f$ is the forward velocity of tracer passing from Cell 1 to 2) indicating further retention of process fluids, the back mixing efficiency presented the lowest square of variance in Cell 1, demonstrated by inefficient mixing in Cell 01 (Table 2). Moreover, both cells presented a mean residence time remained less than the HRT and was similar to that shown at 100% media fill ratio when the media bed was static (Table 2). This again agrees with Wang et al. (2005) that investigated the influence of support media fill ratio in suspended carrier biofilm reactors. A media fill ratio of 50% was found to be optimum for removal of chemical oxygen demand (COD) with efficiencies of 73%, whilst a >70% media fill ratio for $NH_4^+$, was crucial to achieve 52% $NH_4^+$ removal. Rusten et al., 2006 investigated the effect of media fill ratio on treatment efficiency in moving bed biological reactors (MBBRs), concluding that <70% as the optimum media fill ratio for $NH_4^+$ removal. Similarly Pedersen et al., 2015, compared the removal of ($NH_4^+$) in fixed and moving media bed reactors, concluding that static media beds offered significant advantage over moving beds, providing protection of nitrifying bacteria in the biofilm.

It was evident that 25% media fill ratio suffered bacterial detachment due to the low surface charge of and hydrophilic nature of nitrifiers (-0.05 to -0.07 meq.$g^{-1}$ VSS) (Basuvaraj et al., 2012). Moreover the low surface adhesion force of polypropylene media surface (10.5nN), recorded by Stephenson et al., (2012), would have reduced re-attachment of nitrifying bacteria. Therefore resulting in a reduction of $NH_4^+$ removal efficiency to 49%.

### *4.5 Influence of aeration on biofilm scouring*

When the SAF reached stable operation, turbidity (NTU) was recorded for each media fill ratio as the aeration rate was increased from 21.8 to 43.7 $m^3.h^{-1}.Cell^{-1}$. This was performed to measure the influence of aeration on biofilm detachment. Figure 6a shows the

influence of aeration rate on turbidity in Cell 1and Figure 6b in Cell 2. At 100% media fill ratio, Cell 1 shows the lowest turbidity of all studies, remaining below 300 NTU as aeration was increased from 21.8 to 43.7 $m^3.h^{-1}.Cell^{-1}$ (Figure 6a). Therefore an aeration rate of 21.8 $m^3.h^{-1}.Cell^{-1}$ would be considered adequate for biofilm scouring in Cell 1, with little turbidity accumulation (Figure 6a). Turbidity did however accumulate in Cell 2 at 100% media fill ratio when the SAF operated at an aeration rate of 21.8 $m^3.h^{-1}.Cell^{-1}$ displaying a value of 486 NTU. Interestingly, as the aeration rate was increased to 43.7 $m^3.h^{-1}.Cell^{-1}$, air scouring efficiency increased, and turbidity reduced to 308 NTU. This indicates that inactive bacterial material, was removed from the SAF 110 mm holes in the dividing baffles. Table 5 shows the VSS/TSS ration in Cell 1 and 2 but no significant differences were found, indicating that turbidity measurements give slightly different information, as this technique is able to measure finer solids. For a 100% media fill ratio VSS/TSS ratio was 0.85 and 0.86 for Cell 1 and 2 respectively, which was the lowest of all studies, but comparable with activated sludge which operates between 0.7 to 0.85 (Sperling., 2007).

When the SAF operated with a 75% media fill ratio and aeration rate of 21.8 $m^3.h^{-1}.Cell^{-1}$, Cell 1 showed a slight increase in turbidity from 100% media fill ratio at 333 NTU (Figure 6a). Turbidity increased as it passed from Cell 1 to 2 from 333 NTU to 846 NTU respectively at an aeration rate of 21.8 $m^3.h^{-1}.Cell^{-1}$, indicating scoured material accumulated in Cell 2 (Figure 6b). The VSS/TSS ratio at 75% media fill ratio shown in Table 5 for increased to 0.88 in both Cells from 100% media fill ratio, demonstrating an increase in scoured and sloughed material related to the media re-ordering.

A linear increase in turbidity was seen at 50% media fill ratio from 305 to 521 NTU, as aeration rate was increased from 21.8 to 43.7 $m^3.h^{-1}.Cell^{-1}$ (Figure 5a). Therefore air scouring was inefficient and scoured bacterial material was seen to accumulate in Cell 1. The most significant change of all studies occurred in Cell 2 at 50% media fill ratio in, whereby

turbidity increased from 527 to 1800NTU as aeration was increased from 21.8 to 43.7 $m^3.h^{-1}.Cell^{-1}$ (Figure 6b). This agrees with other studies, where heterotrophic bacteria have with their high growth rates, compared to slow growth rate nitrifying bacteria, produced a larger mass of inactive bacterial material (Basuvaraj et al., 2012; Zinatizadeh and Ghaytooli, 2015).

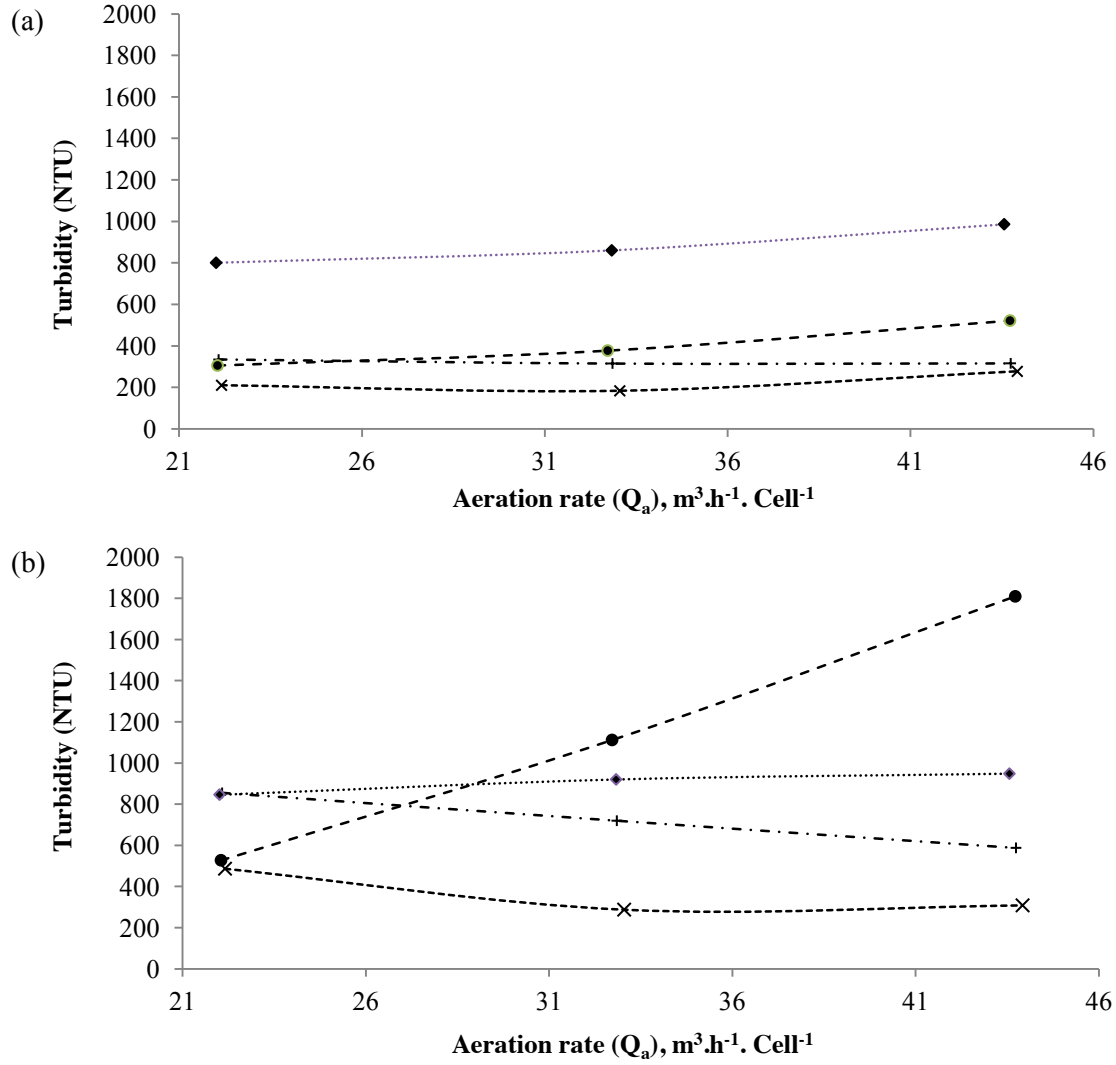


**Figure. 6.** Turbidity (NTU) and aeration rate for 100, 75, 50 and 25 media fill ratios. Where 100% media fill ratio (×), 75% media fill ratio (+), 50% media fill ratio (•) and 25% media fill ratio (♦) in Cell 1 (a) and in Cell 2 (b). The SAF was fed with 2.5 ±0.07 $m^3.h^{-1}$ and aerated between 21.85 and 43.7 $m^3.h^{-1}.Cell^{-1}$.

A linear increase in turbidity was seen at 25% media fill ratio turbidity from 800 to 986 NTU in Cell 1 as aeration increased from 21.8 to 43.7 $m^3.h^{-1}.Cell^{-1}$ (Figure 6a). Similarly Cell 2 increased linearly from 846 to 947 NTU as aeration increased from 21.8 to 43.7 $m^3.h^{-1}.Cell^{-1}$ (Figure 6a). At 25% media fill ratio the VSS/TSS ratio increased from 50% media fill ratio to 0.89 in both Cells, hence the suspended, active fraction of the biomass had increased. This agrees with Jianlong et al., (2000) in experiments on bioreactors where the largest combined concentrations of VSS occurred between 22.5 and 30% media fill ratio. Therefore MLVSS would be a relevant measure SAF performance at media fill ratios below 50%. As identified by Burrows et al., (1999), in studies on activated sludge plants, reactor design should consider washout of bacterial flocs, due to largest *Qr* at 53.46 $m^3.h^{-1}$ for 25% media fill ratio. Thus further research is required to understand the influence of HRT on the washout of bacterial flocs.

**Table 5.** Ratio of VSS to TSS for each media fill ratio for Cell 1 and 2 at an aeration rate of 21.8 $m^3.h^{-1}.Cell^{-1}$. * Average of three sample analyses.

| Parameter | VSS/TSS (Cell 1)* | VSS/TSS (Cell 2)* |
|---|---|---|
| SAF, 100% media fill ratio, Cell 01 | 0.85 | 0.86 |
| SAF, 75% media fill ratio, Cell 01 | 0.88 | 0.88 |
| SAF, 50% media fill ratio, Cell 01 | 0.86 | 0.86 |
| SAF, 25% media fill ratio, Cell 01 | 0.89 | 0.89 |

### *4.6 DO and temperature*

DO and temperate were measured for the influent and effluent from both Cells. Pre-aeration from up-stream trickling filters and fluid agitation in the SAF feed meant influent DO ranged from 7.8 to 9.8 $mg.l^{-1}$, dependent on influent temperature. At 100% media fill ratio the largest consumption of $O_2$ occurred across Cell 1, with a reduction from 9.77 to 8.68 $mg.l^{-1}$ (Figure 7a). Across Cell 2 DO increased to 9.69 $mg.l^{-1}$, indicating a lower DO demand. Influent temperature was 14$^{o}$C at 100% media fill, impacting on $O_2$ solubility (Doran, 2013).

When the media re-ordered at 75% media fill ratio the lowest influent DO occurred at 7.83 $mg.l^{-1}$, but again Cell 1 showed the greatest O2 consumption (Figure 7a). The most significant change in DO occurred at 25% media fill ratio in Figure 7a, where a steep linear increase from 9.26 $mg.l^{-1}$ in the influent, to 10.07 $mg.l^{-1}$ across Cell 1 and 11.59 $mg.l^{-1}$ across Cell 2 occurred, which is close to $O_2$ saturation of 12.05 $mg.l^{-1}$ (Doran, 2013). The largest *Qr* at 25% media fill ratio was observed at 43.6 $m3.h^{-1}$ (Figure 4), along with the high dispersion shown in the D and d at 0.012 and 60.6 respectively. However it should be noted that the lowest influent temperature of 10.8°C and reduction to 8.7°C in Cell 2 effluent increased $O_2$ solubility and reduced bacterial activity.

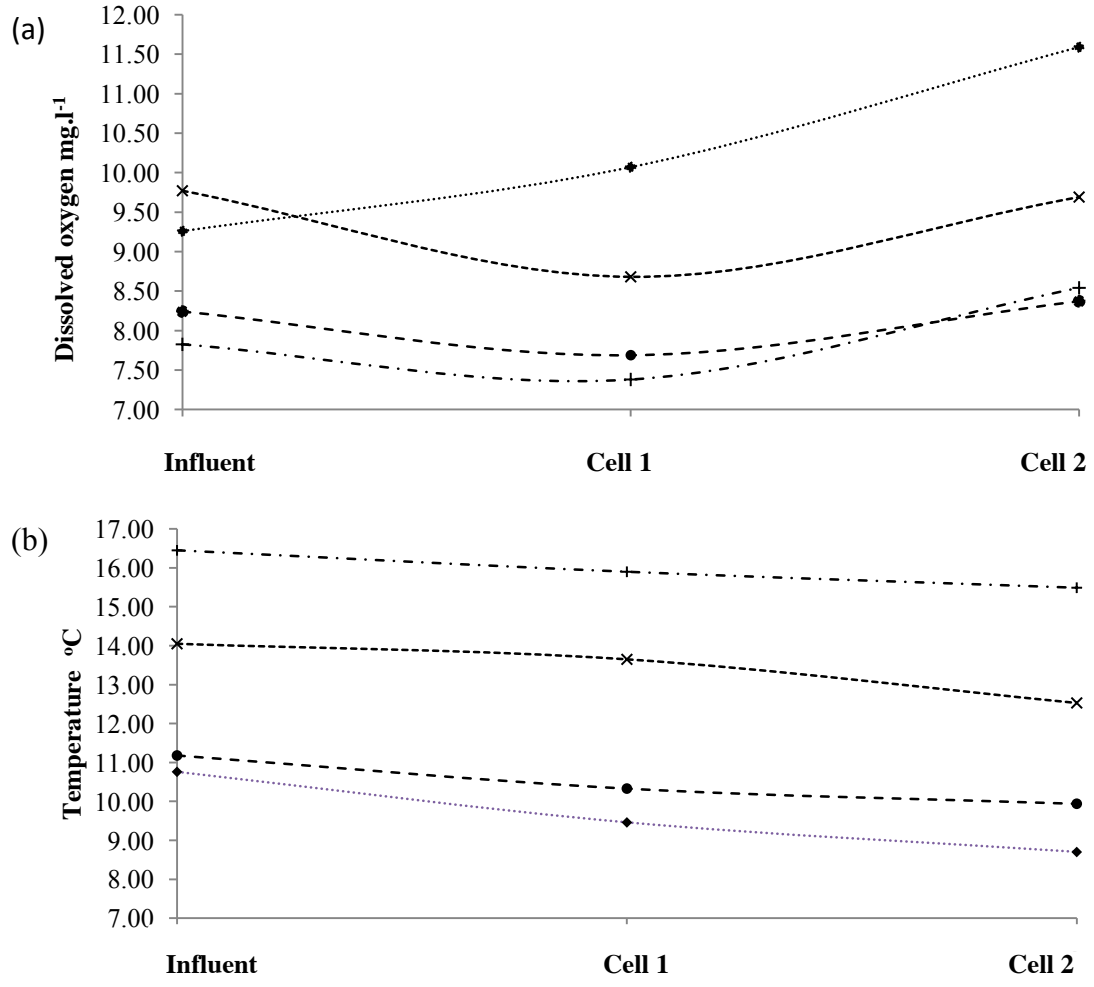

**Figure. 7.** The DO profile for the influent, Cell 1 and Cell 2 *(a)* temperature for the influent, Cell 1 and Cell 2 *(b)* on the SAF with 100% media fill ratio (×), 75% media fill ratio (+), 50% media fill ratio (●) and 25% media fill ratio (♦). The SAF fed at 2.5 ±0.07 $m^3.h^{-1}$ and aerated at 21.85 $m^3.h^{-1}.Cell^{-1}$.

## 5. Conclusions

Internal hydrodynamics directly influences the performance of SAF reactors-which in turn influence fluid retention, dispersion and mass transport. Ultimately these parameters affect mass transfer of $O_2$ into wastewater and diffusion of soluble organics and $NH_4^+$ into the biofilm.

RTD experiments correlated with process performance studies, identifying 100% media fill ratio as the optimum for $NH_4^+$ removal and 50% for $BOD_5$ removal. It was clear from the results that dispersion and tracer retention characteristics, were governed by SAF geometry, media fill ratio, aeration rate, which in-turn influenced the proportion of active biomass. Internal recirculation rate was influenced by media fill ratio, which also affected the efficiency $O_2$ mass transfer with 100% media fill ratio having the largest DO demand. The turbidity experiments identified an accumulation of sloughed and scoured particularly at 50% media fill ratio in Cell 2, when as aeration as increased to 43.7 $m^3.h^{-1}.Cell^{-1}$ the turbidity increased to 1800 NTU.

This research has identified a number of areas to increase knowledge on SAF processes. These areas include analysis of biofilm architecture and morphology in SAF processes to identify favourable fluid velocities for carbonaceous and nitrifying SAF processes. Monitoring internal hydrodynamic conditions and process performance provides far reaching benefits and when used as a diagnosis tool for underperforming SAF processes, informed process changes can be made and initial process design enhanced.

**5. Acknowledgements:**

This research was supported by WPL LTD.

**6. References:**

Ahnert, M., Kuehn, V. and Krebs, P. (2010), "Temperature as an alternative tracer for the determination of mixing charecteristics in wastewater treatment plants.", *Water Research,* vol. 44, pp. 1765-1776.

Albuquerque, A., Makinia, J. and Pagilla, K. (2012), "Impact of aeration conditions on the removal of low concentrations of nitrogen in a tertiary partially aerated biological filter", *Ecological Engineering,* vol. 44, pp. 44-52.

American Water Works Association, ( 1998), *Standard methods for the examination of water and wastewater*, American Waterworks Association, Denver Colorado.

Basuvaraj, M., Lori, L. and Steven, N. L. (2012), "Structural, physicochemical and microbial properties of flocs and biofilms in integrated fixed-film activated sludge (IFFAS) systems", *Water Research,* , no. 46, pp. 5085-5101.

Benthum, W. A. J., Lans, R. G. J. M., Loosedrecht, M. C. M. and Heijnen, J. J. (2000), "The biofilm airlift suspension extension reactor - II: Three phase hydrodynamics", *Chemical Engineering Science*, vol. 55, pp. 699-711.

Bibo, H., Wheatly, A., Ishtchenko, V. and Huddersman, K. (2011), "Effect of shock loads on SAF bioreactors for sewage treatment works", *Chemical Engineering Journal,* vol. 166, pp. 73-80.

Burrows, L. J., Stokes, A. J., West, C. F., Forster, C. F. and Martin, A. D. (1999), "Evaluation of different analytical methods for tracer studies in aeration lanes of activated sludge plants", *Water Research,* vol. 33, pp. 367-374.

Christianson, L., Helmers, M., Bhandari, A. and Moorman, T. (2013), "Internal hydraulics of agricultrual drainage denitrification bioreactor", *Ecological Engineering,* vol. 52, pp. 298-307.

Davidson, J., Helwig, N. and Summerfelt, S. T. (2008), "Fluidised sand biofilters used to remove ammonia, biochemical oxygen demand, total coliform bacteria, and suspended solids from an intensive aquaculture effluent", *Aquacultural Engineering*, vol. 39, pp. 6-15.

Doran, P. M. (2013), *Bioprocess Engineering Principles*, 2nd ed, Elsevier, United Kingdom.

Gálvez, J. M., Gómez, M. A., Hontoria, E. and González, L. J. (2003), "Influence of hydraulic loading and air flowrate on urban wastewater nitrogen removal with a submerged fixed-film reactor", *Journal of Hazardous Materials,* vol. 101, pp. 219-229.

Hodkinson, B. J., Williams, J. B. and Ha, T. N. (1998), "Effects of plastic support media on the diffusion of air in a submerged aerated filter", *CIWEM,* vol. 12, pp. 188-190.

Hu, B., Wheatley, A., Ishtchenko, V. and Huddersman, K. (2011), "The effect of shock loads on SAF bioreactors for sewage treatment works", *Chemical Engineering Journal,* vol. 166, pp. 73-80.

Jianlong, W., Hanchang, S. and Yi, Q. (2000), "Wastewater treatment in a hybrid biological reactor (HBR): effect of organic loading rates", *Process Biochemistry,* vol. 36, pp. 297-303.

Khoshfetrat, A. B., Nikakhtari, H., Sadeghifar, M. and Khatibi, M. S. (2011), "Influence of organic loading and aeration rates on performance of a lab-scale upflow aerated submerged fixed-film bioreactor", *Process Safety and Environmental Protection,* vol. 89, pp. 193-197.

Kilonzo, P. M., Margaritis, A., Bergougnou, M. A., Jun, T. Y. and Qin, Y. (2006), "Influence of baffle clearance design on hydrodynamics of a two riser rectangular airlift reactor with inverse internal loop and expanded gas-liquid separator", *Chemical Engineering Journal,* vol. 121, pp. 17-26.

Lamia, B. G., Christophe, A., Carine, B., Sandrine, A., Xavier, C., Carole, M. J. and Luc, F. (2012), "Modelling of hydrodynamic behavior of a two stage bioreactor with cell recycling dedicated to intensive microbial production", *Chemical Engineering Journal,* vol. 183, pp. 222-230.

Levenspiel, O. (1999), *Chemical reaction engineering,* 3rd ed, J Wiley, US.

Moore, R. E., Quarmby, J. and Stephenson, T. (1999), "BAF media: Ideal properties and their measurement", *Institute of Chemical Engineers,* vol. 77, pp. 291-297.

Moore, R. E., Quarmby, J. and Stephenson, T. (2001), "The effects of media size on the performance of biological aerated filters", *Water Research,* vol. 35, pp. 2514-2522.

Pedersen, L. F., Oosterveld, R. and Pedersen, P. B. (2015), "Nitrification performance and robustness of fixed and moving bed biofilters having identical carrier elements", *Aquacultural Engineering,* vol. 65, pp. 37-45.

Peladan, J., Lemmel, G., Tarallo, H., Tattersall, S. and Pujol, R. (1997), "A new generation of upflow biofilters with high water velocities", *Proceedings of the international confrence on advanced wastewater treatment processes,* Sept 8-11, Leeds United Kingdom, .

Priya, V. S. and Ligy, P. (2015), "Treatment of volitile organic compounds in pharmaceutical wastewater submerged aerated biological filter", *Chemical Engineering Journal,* vol. 266, pp. 309-319.

Regmi, P., Thomas, W., Schafran, G., Bott, C., Rutherford, B. and Waltrip, D. (2011), "Nitrogen removal assesment through nitrification rates and media biofilm accumilation in IFAS demonstration study.", *Water Research,* vol. 45, pp. 6699-6708.

Rexwinkel, G., Heesink, A. B. M. and Swaaji, V. (1997), "Mass transfer in packed beds at low Peclet numbers - wrong experiments or wrong interpretations.", *Chemical Engineering Science,* vol. 52, pp. 3995-4003.

Romero, M. D. C., Lopez, A. L., Rodriguez, V. R. and Becerril, E. L. (2011), "Hydrodynamic and kinetic assesment of an anaerobic fixed-bed reactor for slaughterhouse wastewater treatment", *Chemical Engineering and Processing,* vol. 50, pp. 273-280.

Rusten, B. (1984), "Wastewater treatment with submerged biological filters", *Water Pollutant Control Federation,* vol. 56, pp. 424-431.

Rusten, B., Eikebrokk, B., Ulgenes, Y. and Lygren, E. (2006), "Design and operations of the Kaldnes moving bed biofilm reactors", *Aquacultural Engineering,* vol. 34, pp. 322-331.

Seifert, D. and Engesgaard, P. (2007), "Use of tracer tests to investigate changes in flow and transport properties due to bioclogging of porus media.", *Journal of Contaminant Hydrology,* vol. 93, pp. 58-71.

Sperling., M. V. (2007), *Activated sludge and aerobic biofilm reactors,* IWA publishing, London UK.

Stephenson, T., Reid, E., Avery, L. M. and Jefferson, B. (2012), "Media surface properties and the development of nitrifying biofilms in mixed cultures for wastewater treatment", *Process Safety and Environmental Protection,* vol. 91, pp. 1-4.

Stevens, S. K., Berthouex, P. M. and Chapman, T. W. (1986), "The effect of tracer diffusion in biofilm on residence time distributions", *Water Research,* vol. 3, pp. 369-375.

Tchobanoglous, G., Burton, F. L. and Stensel, H. D. (2003), *Wastewater Engineering: Treatment and Reuse,* 4th ed, McGraw-Hill, Boston.

Teefy, S. (1996), *Tracer studies in water treatment facilities: A protocol and case studies,* 1st ed, AWWA Reaserch Foundation, US.

Wang, R. C., Wen, X. H. and Qian, Y. (2005), "Influence of carrier concentration on the performance and microbial characteristics of a suspended carrier biofilm reactor", *Process Biochemistry,* vol. 40, pp. 2992-3001.

Water Environment Federation (2010), *Biofilm Reactors,* 1st ed, Mc Graw Hill, USA.

Zeng, M., Soric, A. and Roche, N. (2013), "Calibration of hydrodynamic behaviour and biokinetics for TOC removal modeling in biofilm reactors under different hydraulic conditions", *Bioresource Technology,* vol. 144, pp. 202-209.

Zhu, S. and Chen, S. (2001), "Impacts of reynolds number on nitrification biofilm kinetics", *Aquacultural Engineering,* vol. 24, pp. 213-229.

Zinatizadeh, A. A. L. and Ghaytooli, E. (2015), "Simultaneous nitrogen and carbon removal from wastewater at different operating conditions in a moving bed biofilm reactor (MBBR): Process modeling and optimization", *Journal of the Taiwan Institute of Chemical Engineers,* , pp. 1-14.